



Original Article

Influences of sensing positions on principal components and performance of a one-dimensional distributive tactile sensor

Pensiri Tongpadungrod^{1*} and Jaratsri Rungrattanaubol²

¹ *Department of Production Engineering, Faculty of Engineering,
King Mongkut's University of Technology North Bangkok, Bang Sue, Thailand.*

² *Department of Computer Science and Information Technology, Faculty of Science,
Naresuan University, Phitsanulok, 65000 Thailand.*

Received 22 January 2010; Accepted 28 February 2011

Abstract

This paper describes an arrangement of a one-dimensional distributive tactile sensing system that can be used to determine an applied position of a point load of a constant magnitude. The performance of the system was examined using inputs derived from a mathematical model and a back propagation neural network as an interpretation algorithm. Performances of the system with 2–8 inputs with and without an application of principal component analysis (PCA) as a preprocessor were examined. For each number of inputs, four sets of sensing positions were explored and the accuracies in determining an applied load position were compared. It was found that the system was able to determine an applied load position with errors in the range of 1.0–3.1 mm depending on the number of inputs and the method of inputting data. The error decreased with an increase in the number of inputs. It was found that input preprocessing by PCA impaired the performance. Systematically chosen and optimal sets of sensing positions resulted in the most desirable performance and their performances were comparable. Amongst the sets of input positions explored, random positions yielded the highest errors. Random positions also resulted in the largest difference between the first two principal components.

Keywords: neural network, principal component analysis, tactile sensing, position determination

1. Introduction

Force sensing is the fundamental element of tactile sensing information. Early definitions of tactile sensing assumed that the sensed properties must involve the measurement of the contacting force. The development of tactile devices at early stages had been based on force sensing arrangements. As the technology has developed, there has been an increase in the opportunity for devices to be constructed for measuring a wide range of contact properties. As a result, in later publications tactile sensors are referred

to as devices that measure parameters of the interacting contact between the device and certain physical stimuli, such as the size, shape, position, roughness, stiffness, force distribution, and thermal properties (Nicholls and Lee, 1989). Although other stimuli can be used to provide the state of contact, force measurement has remained at the centre of the development of tactile sensing technology as it can be easily interpreted and related to other contact parameters. Most devices rely on an array of numerous sensing elements to infer contact parameters, some even reject devices with a single or few sensing elements as tactile devices, instead, these are described as ‘simple touch’ sensors (Harmon, 1982).

Current application areas of tactile sensing have been in robotics for identifying physical properties and manipula-

* Corresponding author.
Email address: pensiri@kmutnb.ac.th

tion, and as a surface to enhance the vision sensing role in identifying the shape, size, and relative position of contacting objects. In robotic applications, tactile sensors are sometimes integrated with a robot finger or multi-fingers for measuring grasped object profiles such as Howe and Cutkosky (1993), Russell (1990), and Charlebois *et al.* (1999), identifying object materials (Dario *et al.*, 1994), and for determining contacting load and location (Fearing, 1990). Some applications have been devised for controlling and manipulating grasped objects; for example devices for detecting slip such as Eghtedari and Morgan (1989), Canepa *et al.* (1998) and Melchiorri (2000). Evans and Brett (1996) and Brett and Stone (1997) examined an approach to determine contact with soft objects and for adjusting grasping strategy to control deformation. Flat surfaces with array sensors are the focus of several studies to emulate the vision systems for discrimination of 2D (Lueng and Payandeh, 1996) and 3D objects such as Caiti *et al.* (1995) and Holweg and Jongkind (1994). Other tactile sensors for discriminating material properties (Li and Shida, 1997) and for detecting thermal properties (Fearing, 1985) are also available. Applications for tactile sensing in medicine are emerging and are currently receiving significant attention in research. A number of research studies on medical tools for force feedback to surgeons in minimal access therapy have been developed in the early 1990's (Lazeroms *et al.*, 1996; Brett and Stone, 1997 and Zivanovic and Davies, 2000). More examples of tactile systems can be obtained from Lee and Nicholls (1999) which provides an extensive collection of works on tactile systems in the 1990's. The basic structure of a tactile sensor comprises a contact surface acting as a protective layer, sensing elements connected by wiring that may be embedded in a substrate, and a support as shown in Figure 1.

Tactile sensing methods are available in a range from simple point force measuring devices through to very complex multi-sensor array systems, from which it is possible to derive more detailed information of contacting objects. For these devices, the main categories include a simple contact (to simply detect the presence of an object), for detecting force magnitude (including torque, shear, and normal forces), three-dimensional shapes, slip and thermal properties.

A distributive sensor consists of multiple sensing elements arranged in a linear or two-dimensional array. The derivation of contact relies on the relative information obtained at individual sensory locations to create a "signature" or "pattern", which differ from one contact type to

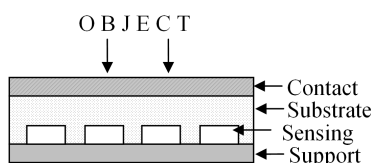


Figure 1. Structure of a tactile sensor.

another. The resolution of a distributive device depends on the interpretation algorithm rather than the number of sensing elements (Brett and Li, 2000). As a result of this, a distributive system has the advantage of having higher spatial resolution than an array sensor of the same number of sensing elements. Distributive sensors are most suited for discrimination tasks; however, they are not ideal to be used to describe the exact shape or location of the contact. The main benefit of the distributive approach is the reduction of the number of sensing elements, in effect a low cost device of simple construction and potentially fast response.

Principal component analysis (PCA) is a statistical technique whereby data in a high-dimensional is reduced to fewer dimensions. The first principal component lies along an axis corresponding with the direction of the largest variation in the data set. The second principal component corresponds with the next largest variance and is orthogonal, and hence is uncorrelated with the first principal component. The derivation of principal components involves the calculation of the eigenvectors (direction) and eigenvalues (magnitude) of the variable data. The derivation of principal components continues until the number of principal components equals the number of input variables. In practice, the need to compute all principal components is rare since the data captured within the first few principal components is usually sufficient to describe the input variables (MacGregor and Kourti, 1995). PCA has been implemented as a data reduction technique, for example, in process fault diagnosis such as MacGregor and Kourti (1995) and Gomm *et al.* (2000) and analysis of benchmarking data (Nickerson and Sloan, 1999). PCA was applied in a distributive tactile sensing system as an evaluator for optimizing sensing positions (Tongpadungrod *et al.*, 2003).

In this paper a simple arrangement of a distributive tactile sensing system is described. The system consists of a thin beam simply supported on both ends. The beam deflection at few locations was detected and used to determine contacting parameters. An applied load position is determined from the beam deflection using a neural network as the interpretation algorithm. Although a closed-form solution for this specific study based on a well established physical model of beam theory is available, the use of neural network is a basis for determination of other physical stimuli for a more complex distributive tactile sensing arrangement (Nicholls and Lee, 1989 and Tongpadungrod *et al.*, 2003). This article aims to examine the effects of applying PCA to beam deflections before used as a neural network input to determine a load position compared to the case where the beam deflections are directly used as inputs. The influences of a change of the location of beam deflection detection are also examined for four sets of locations.

The arrangement of the experimental setup for the system used in this study is described in the next section, followed by description for determining the principal components. In Section 4, the results of load position obtained from neural network are presented. In the same section, the

method to specify the derivation of the sensing location is described. Section 5 compares the system performance in terms of effects of the number of inputs and PCA and effects on sensing positions on the system's accuracy.

2. Experimental Setup and Model

2.1 Experimental setup

A simple experimental tactile sensor was constructed from a one-dimensional surface arranged as a simply supported beam. The distributive surface of the experimental rig was a mild steel beam of the size 400×5×1.2 mm. The supporting structures and sensing elements were mounted on a solid steel base that provided a rigid support. The schematic of the proximity sensing unit are shown in Figure 2. The beam deflection under an applied load was detected at 2-8 positions from which parameters describing the contact could be deduced.

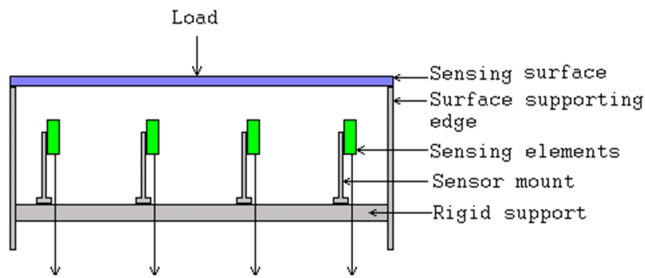


Figure 2. Schematic diagram of the experimental rig.

2.2 Beam theory

The bending theory is reported in most structural mechanics texts, for example Young (1989). The deflection y at position x in response to an applied load P at position a on a simply supported thin beam of length l is given by:

$$y = \frac{P}{6EI} \left[\frac{(2l-a)(a-l)ax + (l-a)x^3}{l} - \langle x-a \rangle^3 \right] \quad (1)$$

where E is the Young's modulus and I is the second moment of inertia. For (1) the following assumptions applied: (a) the beam is straight, (b) the beam is constructed from a homogeneous material of constant elasticity, (c) the cross sectional area remains planar and is uniform, (d) the applied load will not cause permanent deformation, and (e) deflections are small with respect to length. In this study the load was maintained at 3 N.

3. Principal Component Analysis

3.1 Derivation of principal components

The derivation of principal components is carried out as follows (Gomm *et al.*, 2000). For a data set \mathbf{X} , consisting

of beam deflection measured at p sensory positions for N_0 applied positions, the covariance matrix (\mathbf{S}) that describes the relationship of data between sensing elements is:

$$\mathbf{\Sigma} = \frac{1}{N_0} \mathbf{X}^T \mathbf{X} \quad (2)$$

The eigenvectors (\mathbf{U}) and eigenvalues (\mathbf{D}) of \mathbf{S} are solved to satisfy the standard equation:

$$\mathbf{\Sigma} \mathbf{U} = \mathbf{U} \mathbf{D} \quad (3)$$

where \mathbf{D} is a diagonal matrix with the diagonal elements equal to the eigenvalues l_i and $\mathbf{U} = \{\mathbf{U}_1 \dots \mathbf{U}_p\}$ is a matrix whose columns are the normalised eigenvectors such that $\mathbf{U} \mathbf{U}^T = \mathbf{U}^T \mathbf{U} = \mathbf{I}$ (the identity matrix). The eigenvalues l_i correspond to the data variances in the directions of the eigenvectors \mathbf{U}_i . By rearranging the columns of \mathbf{U} in descending order of magnitude of the corresponding eigenvalues, a new matrix \mathbf{U}_p is formed whose p columns are the p principal components of \mathbf{X} .

In summary, the initial input is a matrix of the size $N_0 \times p$ (applied positions \times sensing positions) and is reduced to a $p \times p$ covariance matrix. The covariance matrix illustrates the relationship (correlation) between any two sensing positions from which the eigenvalues (\mathbf{D}) and the eigenvectors (transformation matrix or principal components, \mathbf{U}) of the data set are computed. The derived principal components can be related back to the original beam deflection by transforming the beam deflection using the transformation matrix (eigenvector). The transformation is achieved by deriving the product of the beam deflection and the eigenvectors. As a result, the transformed data is an $N_0 \times p$ matrix the columns of which illustrate the principal components (eigenvectors or shapes) with the influence of the corresponding eigenvalues.

3.2 Principal components of the inputs

PCA was applied to the simulated beam deformation for a set of 10 load positions which were also used for neural network training. The covariance of the input matrix was then calculated using (2). From the covariance matrix, eigenvalues and eigenvectors of the data set were computed according to (3). The eigenvectors were rearranged in a descending order to obtain the principal components matrix \mathbf{U}_p as described earlier. The \mathbf{U}_p matrix was used in transforming the original set of beam deflections to reveal the shape and magnitude of the principal components.

The transformed deflections at eight positions are shown in Figure 3a and 3b. The first principal component corresponded with a distinctively large magnitude. The magnitude of transformed data reduced drastically for later principal components. The magnitudes of the last five principal components were of relatively small significance, such that their corresponding transformed data could not be discerned on the same scale as the first three principal components. The last five principal components are plotted on different scale as shown in Figure 3b. It is likely that the first

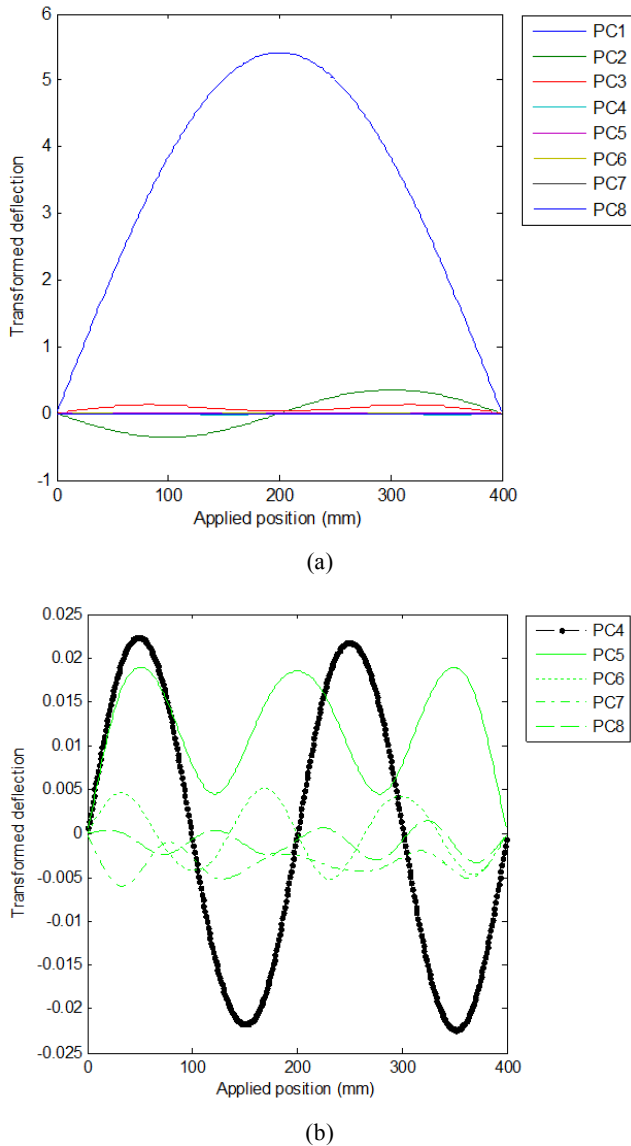


Figure 3. Transformed surface deflection: (a) 1–8 principal components, (b) 4–8 principal components.

principal component is a reflection of the magnitude of deflection whereas the second principal component is influenced by the asymmetry of beam deformation due to an applied load position towards the left or the right of the beam centre. However, the influences of later principal components are less obvious. Throughout the first principal component, it can be seen that the transformed deflection peaked as load was applied close to the beam centre. As for the second principal components, two peaks are observed. The first peak appears mid-section of the left half of the beam and the other appears mid-section of the right half of the beam. Such trend exists for other principal components and it is evident that the number of peaks matches the order of principal components.

By inspection at least two principal components are required for determining an applied position as these give

unique characteristics for all applied positions. However, in practice additional sensing elements to the minimum requirement should be employed for redundancy and to compensate for sensor noise.

4. Determination of Load Position Using Neural Network

An applied load position was deduced from deflections of the beam at specified sensing or input positions using a back propagation neural network as an interpretation algorithm. In this research, a back propagation neural network with sigmoid function was used. The neural network used was developed in-house; however, a commercially available neural network can also be used to obtain the results.

Two methods of inputting data to neural networks were examined. The first method was to directly use deflections at specified sensing positions as the inputs. The other method was to preprocess the deflections through PCA before inputting to the neural networks. For each inputting method, the network was trained with the number of inputs in the range of 2–8 sensing positions. For each number of sensing positions, four sets of sensing positions were explored. The first set of sensing positions (S1) was obtained by dividing the beam into sections equal to the number of inputs and the sensing positions were specified at the midpoint of each section. The second set of sensing positions (S2) was obtained by dividing the beam into sections equal to the number of inputs plus one and the sensing positions were specified at the end of each section. This second set of input positions is a set of sensing positions placement at an equal pitch along the beam length. The third set of sensing positions (S3) was obtained at random. The fourth set of sensing positions (S4) was the optimal positions according to the method described by Tongpadungrod *et al.* (2003). Each training was completed using ten training positions with the load applied at a step of 40 mm along the beam length beginning at 20 mm from the left end of the beam.

Each network consisted of a single hidden layer with ten nodes. For all networks, the momentum rate and the learning rate were fixed at 0.9 and 0.7, respectively. The training process terminated when the compound error reached 10^{-7} or the number of training iterations reached 10^7 . The test data consisted of inputs corresponded to an applied load position at a pitch of 1 mm.

A typical result of determining an applied load position from the beam deflection with and without an application of PCA is as shown in Figure 4, which is an example of prediction using two inputs. Figure 4 shows that the estimate of an applied load position is accurate for most of the beam length in the cases where the inputs were the beam deflections with and without the application of PCA. The estimate of the load position became less accurate as the position approached the restricted ends of the beam. The reason for this could be that load application near the restricted ends resulted in small deflections, which could be difficult for the neural network to provide an accurate output. It should also

be noted that the trained section ranged between 20–380 mm, which corresponded to the section where the accuracy of load determination was satisfactory. In the analysis, the load positions in the same range as the trained section will be included in order to exclude large errors corresponding to the load application near the ends.

5. Comparison of Performances

In this section, the accuracies in determining an applied load positions of networks with the various methods of inputting will be compared.

5.1 Effects of number of inputs and PCA on the performance

The work described in this paper investigated neural network performances over a range of 2–8 inputs. The performances discussed in this section are in the form of (1) the average training error and (2) the average testing error. The average values were obtained from four sets of sensing positions for each number of inputs with and without an application of PCA. Note that the testing errors were calculated only for an applied load within the trained section. The results are as shown in Figure 5 where the horizontal axis is the number of inputs, the vertical axis on the right hand side is the average testing error (mm), and the vertical axis on the left hand side is the average training error.

Figure 4 shows that the average training errors were in the order of 10^{-6} - 10^{-5} . Note that the training goal was such that the training error was at least 10^{-7} or the training reached 10^7 iterations. All networks except one reached the specified number of training iterations before achieving the specified training error. For the same number of iterations, the training error decreased with an increase in the number of inputs. This result suggests that an increase in the number of inputs is beneficial to the convergence of the training error. Figure 5 also shows that the training and testing errors varied in a similar trend.

It can be seen from Figure 5 that the networks were able to determine an applied load positions from as small as two inputs but the accuracy significantly improved with four inputs. For the number of inputs greater than four, the accuracies fluctuated within a small range. This result suggests that the optimum number of inputs should be four such that the system produces a small error and in order to minimise the cost of the system.

The neural network outputs yielded the positional errors in the range of 3.1 to 1.0 mm in the case where the inputs were obtained without an application of PCA, and 2.8 to 1.3 mm in the case where the inputs were obtained with an application of PCA for the number of inputs in the range of 2–8, respectively. Except with two inputs, the errors of the system when the inputs were derived without an application of PCA were of a smaller value than those of a comparable number of inputs derived with an application of PCA. It can be concluded that training without an application of PCA

yields a more desirable performance. To understand the reason for this, we have compared the neural network inputs with and without an application of PCA. An example of the comparison where the network was trained with two inputs at the optimal positions can be seen in Figure 6.

Figure 6 illustrates a comparison of input values for neural network training in the cases where the inputs were derived with and without an application of PCA. The x-axis represents the training set (there are ten sets corresponding to ten applied load positions as described earlier). The y-axis represents the input values. In Figure 6 the sensors were placed at optimal positions (S4). The inputs derived from an application of PCA were pairs of values with a large magnitude and a rather small magnitude. The substantial differences between the magnitudes of the inputs derived from

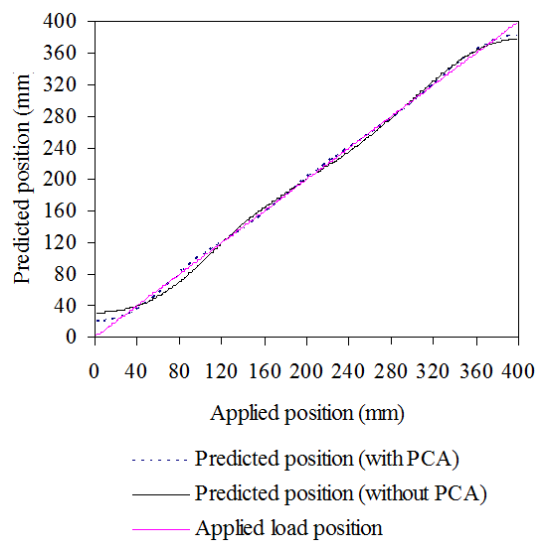


Figure 4. Predicted load position from 2 inputs with and without an application of PCA.

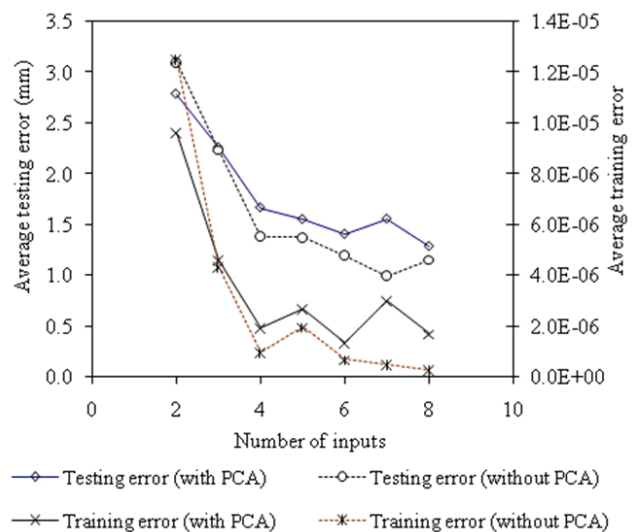


Figure 5. Neural network training and testing errors as a function of number of inputs.

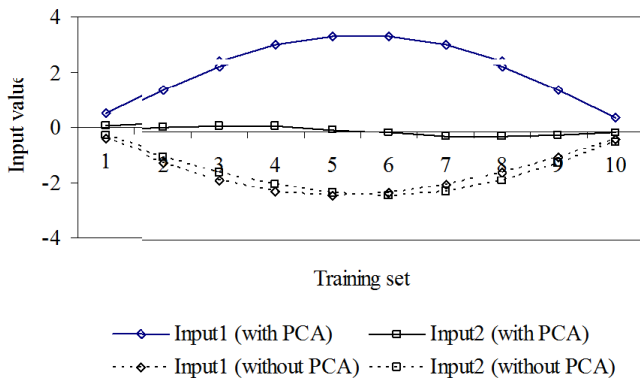


Figure 6. Neural network training with two inputs with and without an application of PCA when the sensors were at optimal positions (X4).

PCA were due to the fact that PCA magnifies the significance of the first principal component through the eigenvalue. As a result, later principal components became smaller in magnitude. It is possible that neural networks became less sensitive to the second principal component used as the input. In contrast, it can be seen that the inputs without an application of PCA were pairs of values that were of similar magnitudes. It is possible to input the data to the neural network using a different method to increase the magnitude of the second principal component.

5.2 Effects of sensing positions on the neural network performance and on the principal components

In this section, the performances of the neural network with different sensing positions will be compared. In addition, we will also consider the principal components at different sensing positions.

The training and testing errors have been used as benchmarks to compare neural network performances with different sensing positions. Both the cases where the inputs were derived with and without an application of PCA will be investigated. The average training and testing errors of all numbers of inputs investigated for each set of sensing positions are shown in Figure 7. In Figure 7, the x-axis represents each set of the sensing positions, the y-axis on the right hand side is the average testing error (mm) and the y-axis on the left hand side is the average training error.

Figure 7 shows that the input sets S1, S2, and S4 yielded similar performances. On average they are more superior in performance than the set S3 both in terms of training and testing. Although the sets S4 were obtained from optimisation, the performances were comparable with the sets S1 and S2, which were positions at an equal pitch. In all cases, the inputs at random positions (S3) generated the highest errors. For all sets of inputs, the testing errors are of the same trend. The result with a large training error also corresponds to the system with a large testing error.

In order to investigate the effects of sensing positions on the principal components, the average values of the principal components of each set of sensing positions were calculated. Because the smallest number of inputs investigated in this study was two inputs, we will compare values of the first two principal components. The results are as shown in Figure 8.

In Figure 8 the x-axis corresponds to the set of sensing positions, the y-axis on the right is the average testing error (mm) and the average value of the first principal component and the y-axis on the left is the average value of the second principal component. The graph shows that the testing error tended to vary in the same direction as the value of the first principal component. In all cases except the case of random sensing position (S3), the testing error tended to vary in the same direction as the value of the second principal component. By inspection, the difference between the first and the second principal components of the set S3 was of the highest value and could have an influence on the performance of the system. To investigate the effect of the difference

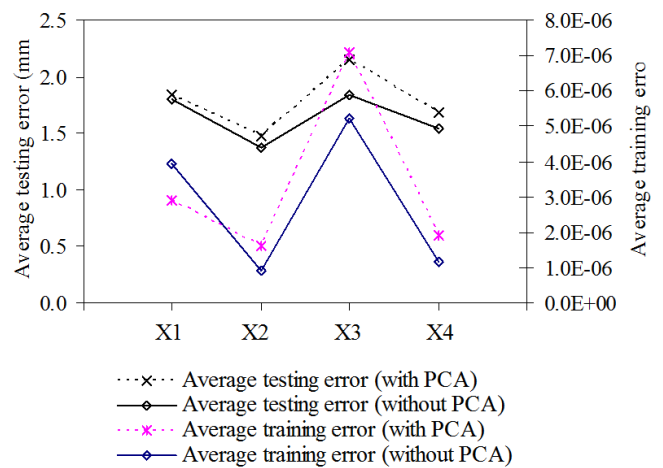


Figure 7. Average training and testing errors with and without an application of PCA for the sets of input positions investigated.

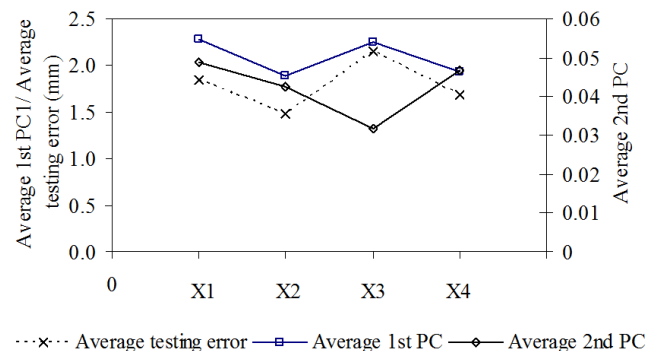


Figure 8. Average values of the first and the second principal components and the input positions.

between the principal components on the performance of the system, average ratio between the first two principal components of the input sets have been obtained. Figure 9 shows a comparison between the ratio as described and the testing errors.

It can be seen from Figure 9 that the average ratio between the first and the second principal components of the set S3 was of the highest value whereas those of the other three sets of inputs were of similar values. The figure also shows that the high ratio value of the input set S3 also corresponded with the high value of the testing error. It should also be noted that the trend of the ratio between the first and the second PCs closely form a similar trend as the magnitude of the first PC.

The work described by Tongpadungrod (2002) successfully used PCA as an evaluator for optimising sensing position of a tactile sensing system. The optimisation goal was based on reduction the eigenvalue of first few PCs. In this work, the relationship between the ratio of the first two PCs and the average testing error which defines the system's performance was explored. An additional study presented in this work suggested that the optimal sensing positions should be specified in such a way that they resulted in a reduction in magnitude of the first PC.

6. Conclusions

The study has shown a system that can be used to determine an applied load position on a one-dimensional surface. An applied load position within the trained section can be determined with satisfactory accuracy using as small as two inputs for a neural network trained with only ten applied load positions. The accuracy was in the range of 3.1–1.0 mm when the inputs were derived with an application of PCA and 2.8–1.3 mm when the inputs were derived without an application of PCA for 2–8 inputs, respectively. The study has shown that the performance becomes more desirable with an increase in the number of inputs and when the inputs were obtained without an application of PCA.

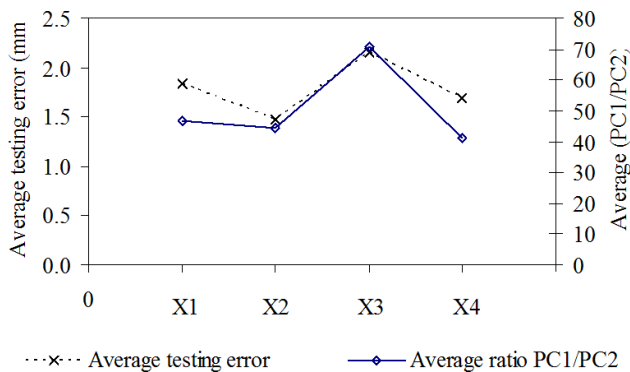


Figure 9. Ratio between the first and the second principal components (PC1/PC2) and the input positions.

Random sensing positions gave the worst performance among the sets of sensing positions under investigation. Systematically chosen sensing positions and optimal sensing positions resulted in similar performance. The random sensing positions gave the largest difference between the first and the second principal components which also corresponds to the least desirable performance.

Acknowledgements

The authors would like to thank the Science and Technology Research Institute of King Mongkut's University of Technology North Bangkok for their financial supports of this work.

References

- Brett, P.N. and Li, Z. 2000. A tactile sensing surface for artificial neural network based automatic recognition of the contact force position. *Proceedings of the Institution of Mechanical Engineers*. 214(I), 207–215.
- Brett, P.N. and Stone, R.W.S. 1997. A technique for measuring contact force distribution in minimally invasive surgical procedures. *Proceedings of the Institution of Mechanical Engineers*. 211(H), 309-316.
- Caiti, A., Canepa, G., De Rossi, D., Germagnoli, F., Magnenes, G. and Parisini, T. 1995. Towards the realization of an artificial tactile system: Fine-form discrimination by a tensorial tactile sensor array and neural inversion algorithms. *IEEE Transactions on Systems, Man, and Cybernetics*. 25(6), 933-946.
- Canepa, G., Petrigliano, R., Campanella, M. and De Rossi, D. 1998. Detection of incipient object slippage by skin-like sensing and neural network processing", *IEEE Transactions on Systems, Man, and Cybernetics*. 28(3), 348-356.
- Charlebois, M., Gupta, K. and Payandeh, S. 1999. Shape description of curved surfaces from contact sensing using surface normals. *International Journal of Robotic Research*. 18(8), 779-787.
- Dario, P., Rucci, M., Guadagnini, C. and Laschi, C. 1994. An investigation of robot system for disassembly automation, In the *Proceedings of: the IEEE International Conference on Robotics and Automation*, San Diego, CA, 8-13 May 1994. *IEEE Robotics and Automation Society*. 3515-3521.
- Eghtedari, F. and Morgan, C. 1989. A novel tactile sensor for robot applications. *Robotica*. 7, 289-295.
- Evans, B.S. and Brett, P.N. 1996. Computer simulation of the deformation of dough-like materials in a parallel plate gripper. *Proceedings of the Institution of Mechanical Engineers*. 210(B), 119-126.
- Fearing, R.A. 1985. Thermal sensor for object shape and material constitution. *Robotica*. 4(4), 31-34.
- Fearing, R.S. 1990. Tactile sensing mechanism. *International Journal of Robotics Research*. 9(3), 3-23.

- Gomm, J. B., Weerasinghe, M. and Williams, D. 2000. Diagnosis of process faults with neural networks and PCA. Proceedings of the Institution of Mechanical Engineers Part E. Journal of Process Mechanical Engineering. 214(2), 131-143.
- Harmon, L.D. 1982. Automated tactile sensing. International Journal of Robotics Research. 1(2), 3-32.
- Holweg, G.M. and Jongkind, W. 1994. Object recognition using a tactile matrix sensor. EURISCON' 94 Advanced Manufacturing and Automation RES 1994, Malaga, Spain, 1379-1383.
- Howe, R.D. and Cutkosky, M.R. 1993. Dynamic tactile sensing-perception of fine surface-features with stress rate sensing. IEEE Transactions on Robotics and Automation. 9(2), 140-151.
- Lazeroms, M., La Haye, A., Sjoerdsma, W., Schreurs, W., Jongkind, W., Honderd, G. and Grimbergen, C. 1996. A hydraulic forceps with force-feedback for use in minimally invasive surgery. Mechatronics. 6(4), 437-446.
- Lee, M.H. and Nicholls, H.R. 1999. Review Article – Tactile sensing for mechatronics - a state of the art survey. Mechatronics. 9(1), 1-31.
- Leung, A. and Payandeh, S. 1996. Application of adaptive neural network to localization of objects using pressure array transducer. Robotica. 14(4), 407-414.
- Li, D. and Shida, K. 1997. Fuzzy algorithm to discriminate material properties using touch sensors. Electrical Engineering in Japan. 118(1), 61-70.
- MacGregor, J.F. and Kourti, T. 1995. Statistical process control of multivariate processes. Control Engineering Practice. 3(3), 403-414.
- Melchiorri, C. 2000. Detection and control using tactile and force sensors: Focused section on sensors. IEEE/ASME Transactions on Mechatronics. 5(3), 235-243.
- Nicholls, H.R. and Lee, M.H. 1989. A survey of robot tactile sensing technology. International Journal of Robotics Research. 8(3), 3-30.
- Nickerson, J.A. and Sloan, T.W. 1999. Data reduction techniques and hypothesis testing for analysis of benchmarking data. International Journal of Production Research. 37(8), 1717 – 1741.
- Russell, R.A. 1990. Tactile sensing of 3 dimensional surface features. Robotica. 8(Apr), 111-115.
- Tongpadungrod, P. 2002. Characteristics of Tactile Sensing Systems. Ph.D. Thesis, University of Bristol, 180 p.
- Tongpadungrod, P., Rhys, T.D.L. and Brett, P.N. 2003. An approach to optimise the critical sensor locations in one-dimensional novel distributive tactile surface to maximise performance. Sensors and Actuator A: Physical. 105, 47-54.
- Young, W.C. 1989. Roark's formulas for stress and strain. International edition. McGraw-Hill Inc, Singapore.
- Zivanovic, A. and Davies, B.L. 2000. Robotic system for blood sampling. IEEE Transactions on Information Technology in Biomedicine. 4(1), 8-14.